available at www.sciencedirect.com

ScienceDirect

journal homepage: www.elsevier.com/locate/biochempharm

Age-dependent changes in the functional expression of two nicotinic receptor subtypes in CA1 stratum radiatum interneurons in the rat hippocampus

Manickavasagom Alkondon, Edna F.R. Pereira, Edson X. Albuquerque *

Department of Pharmacology and Experimental Therapeutics, University of Maryland School of Medicine, Baltimore, MD, USA

ARTICLE INFO

Article history:
Received 9 May 2007
Accepted 15 June 2007

Keywords:
Choline
Methyllycaconitine
Mecamylamine
Alpha-bungarotoxin
Adult rats
glutamate EPSCs

ABSTRACT

Protein density measurements and mRNA analysis have provided valuable information on age-dependent changes in the distribution of different nicotinic receptor (nAChR) subtypes in various areas of the rat brain, including the hippocampus. However, very little is known regarding the functional expression of nAChRs in individual neuron types at various ages. Likewise, there is paucity of information regarding the functional and pharmacological profile of nAChRs in the mature rat hippocampus. To address these issues, we used the whole-cell patch-clamp technique to record nicotinic responses from CA1 stratum radiatum (SR) interneurons in hippocampal slices from rat pups (5–19 days old) and adult rats (2–5 months old). As previously observed in the hippocampus of rat pups, CA1 SR interneurons in the hippocampus of adult rats responded to choline (10 mM, 12 s) with whole-cell currents that decayed to the baseline within the agonist pulse, were sensitive to inhibition by methyllycaconitine (10 nM) or α-bungarotoxin (50 nM), and were, therefore, mediated by α7*[1] [1] nAChRs. Likewise, as previously observed in the hippocampus of young rats, in the adult rat hippocampus excitatory postsynaptic currents (EPSCs) were recorded from SR interneurons in response to a pulse of ACh (0.1 mM, 12 s) applied in the presence of the $GABA_A$ receptor antagonist bicuculline. ACh-triggered EPSCs were inhibited by mecamylamine (1 μM) or choline (1 mM) and were, therefore, likely to have resulted from activation of α3β4β2* nAChR. The magnitude of α7* nAChR-mediated responses increased with the age of the animals. In contrast, the magnitude of α3β4β2* nAChR-mediated responses was highest at the second postnatal week. The distinct age dependency of functional expression of α7* and α3β4β2* nAChRs strongly suggests that the excitability of CA1 SR interneurons is differentially regulated by the nicotinic cholinergic system in the hippocampus of rat pups and adult rats.

© 2007 Published by Elsevier Inc.

[1] According to the nomenclature for nAChRs and their subunits [Lukas RJ, Changeux JP, Le Novere N, Albuquerque, EX, Balfour DJ, Berg, DK et al. International Union of Pharmacology. XX. Current status of the nomenclature for nicotinic acetylcholine receptors and their subunits. Pharmacol Rev 1999; 51: 397–401.], the asterisk next to nAChR subunits throughout text is meant to indicate that the exact subunit composition is not known.

* *Corresponding author*. Department of Pharmacology and Experimental Therapeutics, University of Maryland School of Medicine, 655 W. Baltimore Street, Baltimore, MD 21201, USA. Tel.: +1 410 706 7333; fax: +1 410 706 3991.
E-mail address: ealbuque@umaryland.edu (E.X. Albuquerque).

Abbreviations: nAChR, nicotinic acetylcholine receptor; SR, stratum radiatum; SLM, stratum lacunosum moleculare; ACSF, artificial cerebrospinal fluid; QX-314, lidocaine N-ethyl bromide; MLA, methyllycaconitine; α-BGT, α-bungarotoxin; SO, stratum oriens; SP, stratum pyramidale

0006-2952/$ – see front matter © 2007 Published by Elsevier Inc.
doi:10.1016/j.bcp.2007.06.023

1. Introduction

Nicotinic acetylcholine receptors (nAChRs) in the brain modulate synaptic development and plasticity [2,3]. To date, eight nAChR agonist-binding α (α2–7, 9, 10) subunits and three structural nAChR β (β2–β4) subunits have been cloned from mammalian brain tissue [4]. Different combinations of α and β subunits give rise to functional nAChRs, whereas the α7 nAChR subunits can form functional homomeric nAChRs.

The pharmacological and kinetic properties of various native brain nAChRs have been characterized at the cellular level using primary cultures of neurons from fetal rats, acutely dissociated neurons from rat pups [5–7], and neurons in brain slices obtained from rat pups [8–10]. Pharmacologically and kinetically, three nAChR subtypes, i.e. α7*, α4β2* and α3β4β2* nAChRs, have been identified and well-characterized in hippocampal slices from rat pups [8,11–13]. The α7* nAChRs subserve rapidly desensitizing, type IA responses, which can be fully activated by ACh or choline, and are sensitive to inhibition by nanomolar concentrations of methyllycaconitine (MLA) or α-bungarotoxin (α-BGT). The α4β2* nAChRs give rise to slowly desensitizing, type II responses, which can be activated by ACh, but not by choline, and are sensitive to blockade by 10 μM dihydro-β-erythroidine but not by 10 nM MLA. The α3β4β2* nAChRs can be fully activated by ACh and only partially by choline. Activation of α3β4β2* nAChRs, which is inhibited by 1 μM mecamylamine or by low concentrations of choline, results in AMPA and NMDA receptor-mediated EPSCs, referred to as type III responses. Although choline is known to inhibit all three nAChR subtypes in the hippocampus, the rank order of potency of choline to inhibit different nAChRs is: type III > type IA > type II, with respective IC50s being 15 μM, 37 μM, and 370 μM [13]. In the CA1 field of the hippocampus of rat pups, α7* nAChRs are expressed by most SR interneurons, α4β2* nAChRs are expressed by all stratum lacunosum moleculare (SLM) interneurons and by a small percent of SR interneurons, and α3β4β2* nAChRs are present in glutamate neurons/axons that innervate CA1 SR interneurons. All three nAChR subtypes contribute to the excitatory action of ACh on CA1 SR interneurons [11,14], but it is unclear whether the presence of three nAChR subtypes controlling the excitability of a single neuron type represents a functional redundancy or a specific functional design.

Studies in adult rodents and primates have provided evidence that nAChRs in the hippocampus, including α7* and α4β2* nAChRs, regulate normal cognitive functioning [15]. Furthermore, disruption of α7* nAChR expression/function in the human hippocampus has been shown to correlate well with attentional impairments observed in schizophrenia [16]. Yet, it is hitherto unknown whether the functional nAChR subtypes present in different neurons in the hippocampus of rat pups and adult rats are the same because the characterization of functional nAChRs has been done mostly in the hippocampal slices obtained from preadolescent rats (see Table 1). In fact, studies on adult rats have been limited to the investigation of the effects of nicotinic ligands on synaptic transmission in slices from the hippocampus and nucleus accumbens [17,18], and on hippocampal oscillatory activity in anesthetized rats [19].

Either mRNA measurements or protein binding density revealed that the expression of different nAChR subunits increases transiently during development and declines from early postnatal periods up to adulthood [20–22]. Whether such age-related changes in protein and mRNA expression are

Table 1 – Age and strain of rats used and type of nicotinic responses assessed in various studies on CA1 neurons of acute hippocampal slices

Study #	Rat strain	Age range (postnatal days)	Type of nAChR studied	Reference
1	Sprague–Dawley	8–24	Type IA, type II	Alkondon et al. [41]
2	Wistar	12–18	Type IA	Jones and Yakel [10]
3	Sprague–Dawley	18–27	Type IA	Frazier et al. [9]
4	Sprague-Dawley	15–30	Type IA, type II	Alkondon et al. [8]
5	Not defined	16–54	Type IA, type II	McQuiston and Madison [42]
6	Sprague–Dawley	18–25	Type IA	Hefft et al. [32]
7	Wistar	11–19	Type IA, type II	Sudweeks and Yakel [43]
8[a]	Sprague–Dawley	18–27	Type IA	Buhler and Dunwiddie [44]
9	Sprague–Dawley	16–18	Type IA, type II, type III	Alkondon et al [14]
10[b]	Wistar	1–5	Type IA	Maggi et al. [45]
11	Sprague–Dawley	25–32	Type IA	Thinschmidt et al. [46]
12[c]	Sprague–Dawley	3–30 months	Undefined	Potier et al. [18]
13	Sprague–Dawley	16–27	Type IA	Chang and Fischbach [47]
14	Sprague–Dawley and August Copenhagen Irish	10–23	Type IA, type II, type III	Alkondon et al. [48]
15	Sprague–Dawley	5–141	Type IA, type III	Present study

Type IA response refers to a fast-inactivating nicotinic current that is elicited by the application of ACh or choline, and is blocked by 10–50 nM MLA or 50 nM α-BGT. Type II response refers to a slowly inactivating nicotinic current elicited by the application of ACh but not choline, and is blocked by 10 μM dihydro-β-erythroidine but not by 50 nM α-BGT or 10 nM MLA. Type III response refers to ACh- or DMPP-induced AMPA or NMDA EPSCs, and is blocked by 1 μM mecamylamine but not by 10 nM MLA.

[a] Type IA response in this study refers to ACh-induced GABAergic IPSCs that are sensitive to inhibition by 75 nM MLA.

[b] Type IA response in this study refers to nicotine-induced AMPA EPSCs in CA1 pyramidal neurons.

[c] Nicotinic response in this study refers to cholinergic afferent stimulated- or cytisine-stimulated GABAergic IPSCs.

accompanied by similar changes in nAChR function in individual neuron types remains to be determined. Thus, the present study was designed to examine pharmacologically whether the same nAChR subtypes regulate the excitability of CA1 SR interneurons in the hippocampus of rat pups and adult rats and to evaluate whether the level of activity of these nAChRs changes with the age of the rats.

2. Methods

2.1. Hippocampal slices

Timed-pregnant Sprague–Dawley rats were purchased from Zivic Miller Laboratories (Newcastle, PA) at least 5 days before delivery of the pups. The pregnant rats were housed one per cage in a 12-h light and dark cycle and were allowed free access to food and water. The date of birth was considered to be day 0 (P0). Male rats at ages ranging between P5 and P141 were used in this study. Rats at ages between 59 and 141 days (2–5 months) were considered as young adults. Animal care and handling were done strictly in accordance with the guidelines set forth by the Animal Care Committee of the University of Maryland. Rats were killed by CO_2 narcosis followed by decapitation. Their brains were removed in ice-cold artificial cerebrospinal fluid (ACSF), which was composed of (in mM): NaCl, 125; $NaHCO_3$, 25; KCl, 2.5; NaH_2PO_4, 1.25; $CaCl_2$, 2, $MgCl_2$, 1; and glucose, 25. A sucrose-containing ACSF (composition in mM: sucrose, 230; KCl, 1; NaH_2PO_4, 1.25; $NaHCO_3$, 30; $CaCl_2$, 1; $MgCl_2$, 7; glucose, 25) was used during the cutting of adult rat hippocampal slices. Slices of 250–275-μm thickness were cut using a Vibratome and stored at room temperature in an immersion chamber containing ACSF bubbled with 95% O_2 and 5% CO_2. Whole-cell patch-clamp experiments were performed on visually identified CA1 SR interneurons of rat hippocampal slices. Additionally, biocytin labeling was used to identify the neurons morphologically [23].

2.2. Electrophysiological recordings

Whole-cell currents were recorded from the soma of SR interneurons according to the standard patch-clamp technique using an LM-EPC7 amplifier (List Electronic, Darmstadt, Germany). The slices were superfused with ACSF at 2 ml/min in the presence of the muscarinic antagonist atropine (0.5 μM) and the $GABA_A$ receptor antagonist bicuculline (10 μM). Agonists were applied via a U-tube, and other drugs were applied via bath superfusion. Signals were filtered at 3 kHz and either recorded on a videotape recorder for later analysis or directly sampled by a microcomputer using the pCLAMP9 program (Axon Instruments, Foster City, CA). Patch pipettes were pulled from borosilicate glass capillary (1.2-mm outer diameter), and when filled with internal solution had resistance between 3 and 5 MΩ. The series resistance ranged from 8 to 20 MΩ. At −68 mV, the leak current was generally between 50 and 150 pA, and when it exceeded 200 pA, the data were not included in the analysis. The internal pipette solution contained 0.5% biocytin in addition to (in mM): ethylene-glycol bis(β-amino-ethyl ether)-N-N′-tetraacetic acid, 10; HEPES, 10; Cs-methane sulfonate, 130; CsCl, 10; $MgCl_2$, 2; and lidocaine N-ethyl bromide (QX-314), 5 (pH adjusted to 7.3 with CsOH; 340 mOsm). Membrane potentials were corrected for liquid junction potentials. All recordings were done at room temperature (20–22 °C). Only a single neuron was studied in a given slice, therefore the number of neurons represents the number of hippocampal slices analyzed.

2.3. Data analysis

The frequency of AMPA EPSCs was analyzed using WinEDR V2.3 (Strathclyde Electrophysiology Software, Glasgow, Scotland). The peak amplitude of nicotinic currents and the net charge of NMDA receptor-mediated EPSCs and nicotinic currents were analyzed using the pCLAMP9 software. Typically, the net charge of agonist-evoked responses was calculated for the duration of the agonist pulse starting from the valve opening. Results are presented as mean ± SEM, and compared for their statistical significance by one sample *t*-test or nonparametric ANOVA followed by Dunn's multiple comparison test.

2.4. Drugs used

ACh chloride, atropine sulfate, (−)bicuculline methiodide, choline chloride, glycine, lidocaine N-ethyl bromide (QX-314), and NMDA were obtained from Sigma Chemical Co. (St. Louis, MO). (±)Mecamylamine.HCl was a gift from Merck, Sharp & Dohme Research Laboratories (Rahway, NJ). Methyllycaconitine citrate (MLA) was a gift from Professor M.H. Benn (Department of Chemistry, University of Calgary, Alberta, Canada). Stock solutions of all drugs were made in distilled water.

3. Results

3.1. CA1 SR interneurons in adult rat hippocampus express functional α7* nAChRs

The adult male rats used in this study were between 59 and 141 days old and weighed between 350 and 550 g. U-tube application of a saturating concentration of choline (10 mM) to interneurons held at −68 mV induced whole-cell currents that decayed to the baseline within the agonist pulse and were inhibited by nanomolar concentrations of MLA and α-BGT (Fig. 1A–C). Bath exposure of the hippocampal slices to 1 nM MLA produced partial inhibition, and to 10 nM MLA or 50 nM α-BGT produced near complete inhibition of choline-evoked currents (Fig. 1A–C, and E). The degree of inhibition produced by both MLA and α-BGT was statistically significant ($p < 0.01$ MLA, 1 nM; $p < 0.0001$ MLA 10 nM and α-BGT 50 nM by one sample *t*-test; $n = 3$ neurons each from a total of 6 rats). The duration for maximum reversal of the MLA-induced inhibition of choline-evoked currents was 40 min (MLA, 1 nM) and 60 min (MLA 10 nM) after wash with ACSF. No reversal of inhibition by α-BGT (50 nM) of choline-evoked currents was evident after washing the slices with α-BGT-free ACSF. These currents have the same kinetic and pharmacological profile as choline-evoked currents mediated by α7* nAChRs in CA1 SR interneurons in hippocampal slices of rat pups and are herein referred to as type IA currents. The peak amplitude of choline-

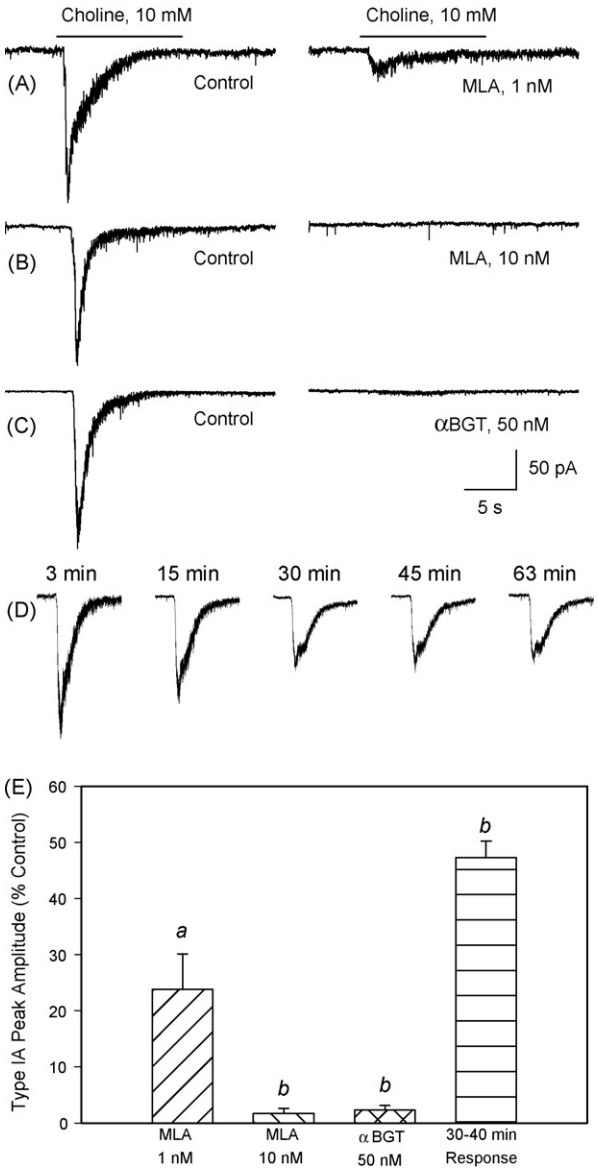

Fig. 1 – Pharmacological analysis of choline-evoked currents in CA1 SR interneurons in the adult rat hippocampus. (A–D) Sample whole-cell current recordings from CA1 SR interneurons of hippocampal slices obtained from adult rats. In each neuron, U-tube application of choline (solid lines at the top of traces) induced fast-decaying type IA nicotinic currents. A 10-min bath exposure of slices to MLA inhibited choline-evoked currents partially at 1 nM (A), and completely at 10 nM (B). A 10-min bath exposure to 50 nM α-bungarotoxin (α-BGT) also completely inhibited the responses (C). Under control conditions, the peak amplitude of choline-evoked currents decreased with recording time (D). (E) Quantitative analysis of the effects of different antagonists on choline-evoked currents and of the rundown of the current amplitudes. The peak amplitude of type IA currents in the presence of MLA was normalized to the mean amplitude of choline-evoked currents recorded right before the exposure to MLA and at 45-min after wash of the slices with MLA-free solution. The peak amplitude of type IA currents in the presence of α-BGT was normalized to the amplitude of currents recorded right before the exposure of the slices to the toxin. The response remaining after 30–40 min was normalized to initial control. Graph and error bars represent mean and S.E.M, respectively, of results obtained from 14 neurons from 10 rats (n = 3 for 1 nM MLA, 3 for 10 nM MLA, 3 for 50 nM α-BGT, and 5 for 30–40-min response). [a]$p < 0.01$; [b]$p < 0.0001$ by one sample t-test. Membrane potential = −68 mV. ACSF contained 0.5 μM atropine and 10 μM bicuculline in all experiments.

evoked type IA currents recorded from adult rat CA1 SR interneurons declined with time during repeated agonist pulses applied every 7–10 min, and stabilized to about 50% of the initial amplitude at 30–40 min of recording (n = 5 neurons from 4 rats; Fig. 1D and E).

Type IA currents were evoked in 19 out of 19 (100% incidence) CA1 SR interneurons studied in hippocampal slices from 15 adult rats (see Table 2). Most of the CA1 SR interneurons (13 out of 19) that responded to choline with type IA currents had their dendrites and axons distributed only in the SR region as evidenced from the images of biocytin-filled neurons (see Fig. 2D). Some SR interneurons (6 out of 19) had their dendrites in the SR but their axons were seen in both the SR and the stratum oriens.

3.2. *Age-dependent changes in the magnitude of α7* nAChR responses recorded from CA1 SR interneurons*

At postnatal day 5 (P5), type IA currents were detected in all 10 neurons studied. However, the peak amplitudes of choline-evoked type IA currents recorded from neurons in slices of P5 rats were small compared to those recorded from neurons in slices of adult rats (Fig. 2A and B). On average, the mean peak amplitude at P5 was about 18% of the adult level. The peak amplitude of type IA current increased progressively with age between P5 and P63, and no further increase was evident at P90 (Fig. 2B). The average peak amplitude of type IA current was 28 ± 10.6 pA at P5 (10 neurons from 6 rats), 43 ± 11.1 pA at P10 (15 neurons from 11 rats), 56 ± 9.2 pA at P15 (29 neurons from 17 rats), 98.1 ± 31.2 pA at P17 (15 neurons from 9 rats), 165 ± 28.1 pA at P63 (8 neurons from 7 rats), and 148.2 ± 25.7 pA (8 neurons from 8 rats). The mean peak amplitude of type IA currents was significantly lower at P5 ($p < 0.01$), P10 ($p < 0.01$) and P15 ($p < 0.05$) compared to P63 or P90 according to nonparametric ANOVA (Fig. 2B).

The age-dependent increase in the amplitudes of type IA currents could have been due to the normal increase in the size of the hippocampus with age and, therefore, the increase in dendritic length and branching. Although the size of hippocampal slices increased with age (see Fig. 2D), the mean capacitance of the CA1 SR interneurons – a measure indicative of their surface area – did not increase to any significant extent with age (see Table 2). Consequently, the current density (pA/pF) values revealed similar age dependency as the current amplitude (Fig. 2B). The net charge of type IA currents also increased with the age of the animals (Fig. 2C) primarily because of the age-dependent enhancement of the amplitudes of type IA currents. The decay-time constants of the currents

Table 2 – Characteristics of nicotinic responses recorded in CA1 SR interneurons

Parameter	Age Groups					
	5 days	10 days	15 days	17 days	19 days	Adult
Mean age (days) (Range)	5.0	10.4 ± 0.22 (8–12)	15.7 ± 0.1 (15–16)	17.6 ± 0.1 (17–18)	19.2 ± 0.15 (19–20)	77.4 ± 5.5 (59–141)
Capacitance (pF)	18.9 ± 1.9	23.4 ± 1.4	22.5 ± 0.9	21.3 ± 1.0	25.4 ± 2.2	21.2 ± 1.7
Incidence of type IA currents (%)[a]	10/10 (100)	15/17 (88.2)	29/29 (100)	15/16 (93.8)	–	19/19 (100)
Incidence of type III response (%)[a]	8/8 (100)	47/47 (100)	24/25 (96)	48/48 (100)	16/17 (94.1)	9/10 (90.0)
Decay-time constant of type IA current (ms)	1175 ± 154	1562 ± 263	1415 ± 114	1826 ± 298	–	1301 ± 151

Data are presented as mean ± SEM.

[a] Numerator indicates number of neurons showing positive responses and denominator indicates the number of neurons studied. The criteria for positive responses were peak amplitude > 5 pA for type IA current, and net charge of ACh-induced NMDA EPSCs > 50 pC for type III response.

did not change significantly with the age of the animals ($p = 0.54$ according to nonparametric ANOVA; Table 2).

3.3. CA1 SR interneurons in the adult rat hippocampus receive glutamatergic inputs that are regulated by type III nAChRs

In the continuous presence of bicuculline, ACh (0.1 mM) evoked EPSCs that could be recorded from CA1 SR interneurons of adult rat hippocampal slices. In neurons voltage clamped at −68 mV, ACh (0.1 mM) induced bursts of EPSCs (Fig. 3A) that were mediated primarily by AMPA receptors as they were sensitive to inhibition by the AMPA receptor antagonist CNQX (10 μM, data not shown). ACh-triggered AMPA EPSCs recorded at −68 mV were clearly detected when the agonist-induced type IA current was inhibited by 10 nM MLA (Fig. 3A, bottom trace) or when the magnitude of ACh-elicited type IA current was small (Fig. 3B and C). In contrast to ACh, choline at a concentration that would have fully activated α7* nAChRs induced only few AMPA EPSCs (see traces in Fig. 1A–C), indicating the involvement of non-α7 nAChR in inducing AMPA EPSCs. In CA1 SR interneurons of adult rat hippocampal slices, a 12-s pulse of ACh (0.1 mM) increased the frequency of AMPA EPSCs from 0.11 ± 0.024 Hz to 1.10 ± 0.265 Hz (7 neurons from 5 rats). ACh was less effective in inducing AMPA EPSCs in presence of 1 μM mecamylamine (Fig. 3B). Similarly, bath application of choline (1 mM) was very effective in inhibiting ACh-induced AMPA EPSCs (Fig. 3C), the inhibitory effect of choline suggests that the release of glutamate by ACh is mediated by type III nAChRs.

ACh-induced EPSCs recorded from CA1 SR interneurons voltage clamped at +40 mV were largely inhibited by the NMDA receptor antagonist APV (50 μM, data not shown), and, were, therefore, primarily mediated by NMDA receptors. U-tube application of ACh (0.1 mM) induced multiple NMDA EPSCs, the high frequency of which resulted in superimposed outward currents (Fig. 4). Thus, instead of analyzing the frequency of NMDA EPSCs, the net charge of superimposed outward currents was taken as a quantitative measure of the net activation of type III nAChRs. The magnitude of ACh-activated NMDA EPSCs was significantly decreased following a 10-min perfusion of the slices with ACSF containing 1 μM mecamylamine (Fig. 4A and C). On average, mecamylamine produced about 57% reduction (4 neurons from 4 rats) of the net charge of ACh-induced NMDA EPSCs (Fig. 4C). The inhibitory effect of mecamylamine remained statistically significant ($p < 0.006$ according to one sample *t*-test). The blocking effect of mecamylamine was reversed after 20–30 min wash with mecamylamine-free ACSF. Following a 10-min perfusion of the slices with ACSF containing 1 mM choline (2 neurons from 2 rats), 12-s pulses of ACh did not evoke NMDA EPSCs (Fig. 4B and C). The blocking effect of choline was reversed after 20–30 min wash of the slices with choline-free ACSF.

Pharmacologically, ACh-induced AMPA and NMDA EPSCs recorded from CA1 SR interneurons in hippocampal slices of young adult rats resembled those previously studied in the hippocampus of rat pups [24,14]. Thus, the failure of 10 nM MLA and the ability of 1 μM mecamylamine or 1 mM choline to inhibit ACh-induced AMPA and NMDA EPSCs suggest that this nicotinic response results from activation of α3β4β2* nAChRs in glutamatergic neurons/axons synapsing onto the interneurons under study.

3.4. Age-dependent changes in the magnitude of type III nAChR responses in CA1 interneurons

The percentage of CA1 SR interneurons that responded to ACh with type III nicotinic responses did not change with the age of the rats (Table 2). However, the magnitude of ACh-induced NMDA EPSCs was largest at the second postnatal week (Fig. 5A). Analysis of the net charge of ACh-induced NMDA EPSCs from several neurons revealed that with the exception of first 2 postnatal weeks, adult level of type III nAChR response was present at a wide range of ages between 15 days and adulthood (Fig. 5B and C). The average net charge of ACh-induced NMDA EPSCs was 499 ± 146 pC at P5 (8 neurons from 5 rats), 600 ± 91 pC at P10 (47 neurons from 25 rats), 276 ± 84 pC at P15 (24 neurons from 17 rats), 237 ± 28 pC at P17 (48 neurons from 30 rats), 291 ± 71 pC at P19 (16 neurons from 9 rats), and 274 ± 50 pC at P69 (9 neurons from 9 rats). The mean net charge of ACh-induced NMDA EPSCs was significantly higher ($p < 0.01$ according to nonparametric ANOVA) at P10 compared to P15 and P17 (Fig. 5B). While the functional expression of type IA nAChRs in CA1 SR interneurons increased with the

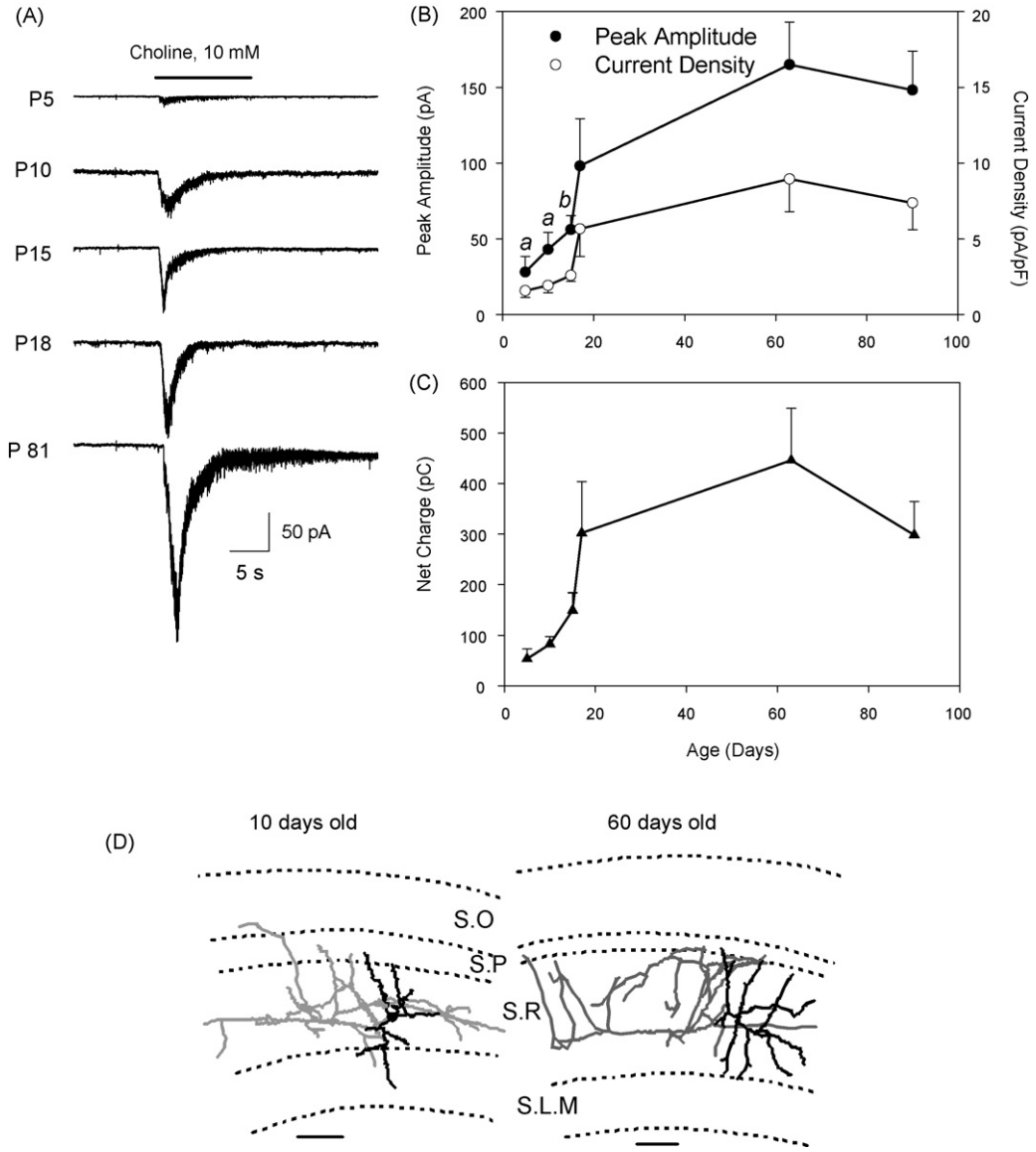

Fig. 2 – Age-dependent changes in the magnitude of type IA currents. (A) Sample type IA currents recorded from CA1 SR interneurons of hippocampal slices obtained from rats of different ages. Note an increase in the peak amplitude with age. (B) Age-dependent changes in the peak amplitude and current density in the type IA current are shown. Each symbol and error bars represent mean and SEM, respectively, of results obtained from 85 neurons from 58 rats (n = 10 for P5; 15 for P10; 29 for P15; 15 for P17; 8 for P63 and 8 for P90). $^{a}p < 0.01$; $^{b}p < 0.05$, compared to P63 and P90 according to nonparametric ANOVA. Rats at ages between 59 and 67 were grouped as P63. Rats at ages between 73 and 141 were grouped as P90. (C) Age-dependent changes in the net charge of type IA currents from the same neurons as in (B). (D) Sample neurolucida drawings of biocytin-filled neurons in hippocampal slices that exhibited type IA currents. Dendrites are in black and axon in grey. Calibration bar = 100 μm. SO, stratum oriens; SP, stratum pyramidale; SR, stratum radiatum; SLM, stratum lacunosum moleculare.

age of the rats reaching near adult levels at third postnatal week, that of type III nAChRs was high during the 2 first weeks after birth and declined to near adult level at third postnatal week (Fig. 5C).

To test whether age-dependent changes in the magnitude of type III responses were a result of age-dependent changes in the NMDA receptor density or in the number of NMDA synapses, we analyzed the magnitude of NMDA evoked currents and sucrose-evoked NMDA EPSCs recorded from CA1 SR interneurons in hippocampal slices from rats at P10 and P17, ages at which significant differences in the magnitude of type III response were noticed (see Fig. 5).

To estimate whether the number of readily releasable glutamatergic vesicles changes significantly with the age of the rats, we applied a short pulse of sucrose to the area including and surrounding the interneurons under study. Sucrose has been shown to trigger transmitter release from synaptic terminals in a Ca^{2+}-independent manner [25,26]. All

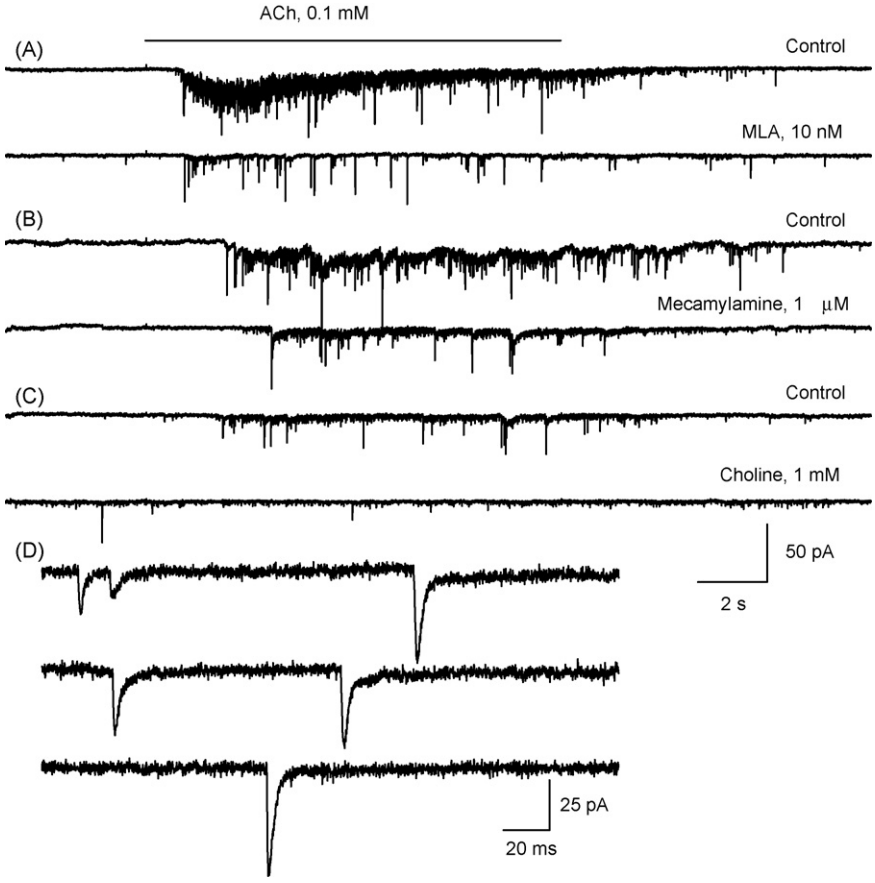

Fig. 3 – Pharmacological analysis of ACh-induced AMPA EPSCs in adult rat hippocampal CA1 SR interneurons. (A) U-tube application of ACh induced type IA current accompanied by AMPA EPSCs. Bath exposure of the slice to 10 nM MLA for 10 min abolished type IA current, but ACh-induced AMPA EPSCs remained. (B) In another SR interneuron, ACh induced lot of AMPA EPSCs that are markedly reduced in number after exposure of the slice to 1 μM mecamylamine for 10 min. (C) In a third SR interneuron, ACh-induced AMPA EPSCs were abolished after 10 min exposure of the slice to 1 mM choline. (D) ACh-induced AMPA EPSCs sampled from the bottom trace in (A) are shown in an expanded scale. Membrane potential = −68 mV.

recordings were obtained in the presence of bicuculline from CA1 SR interneurons voltage clamped at +40 mV, conditions under which sucrose-evoked currents are the result of glutamate release activating NMDA receptors in the neurons under study [12]. As illustrated in Fig. 6, the net charge of the sucrose-induced NMDA currents (5 neurons from 4 rats) did not vary significantly between P10 and P17. Likewise, the net charge of whole-cell currents evoked by U-tube application of the admixture of NMDA (50 μM) and glycine (10 μM) (4 neurons from 3 rats) to CA1 SR interneurons voltage clamped at +40 mV did not change significantly with the age of the animals (Fig. 6A–C). These results suggest that neither the NMDA receptor density nor the NMDA synapse density accounts for age-related changes in type III nAChR responses.

4. Discussion

The results presented herein reveal that at different ages, the majority of CA1 SR interneurons in the rat hippocampus express an nAChR that has the kinetic and pharmacological profiles of type IA, α7* nAChRs. Thus, independent of the age of the animals, most of the CA1 SR interneurons responded to the α7* nAChR agonist choline with fast-desensitizing currents that were sensitive to inhibition by nanomolar concentrations of MLA or α-BGT. Also independent of the age of the rats, CA1 SR interneurons were found to receive glutamatergic inputs whose activity was regulated by receptors pharmacologically characterized as type III, α3β4β2* nAChRs. These observations suggest that the subunit composition of type IA and type III nAChRs does not change with the age of the rats. Whereas α7* nAChR responses in the interneurons increased as a function of age from first postnatal week to adulthood, α3β4β2* nAChR-mediated responses were highest during the first 2 postnatal weeks declining to nearly adult levels at third postnatal week.

The novelty of the present study lies on the functional and pharmacological characterization of α7* and α3β4β2* nAChRs in neurons of the adult rat hippocampus, and on the identification of the age dependency of the magnitude of these two nAChR responses. With the exception of a single study [42] in which the authors used rats at ages between 16 and 54 postnatal days, most studies on α7* and α4β2* nAChR currents were carried out in hippocampal slices obtained from pre-adolescent rats between 1 and 32 days after birth (Table 1).

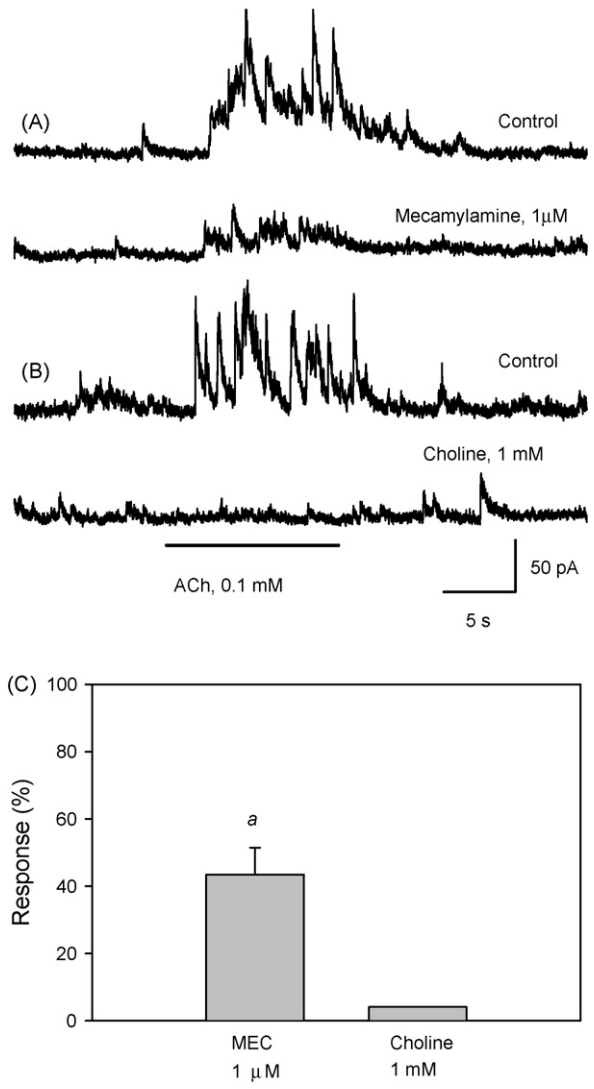

Fig. 4 – Pharmacological analysis of ACh-induced NMDA EPSCs in adult rat hippocampal CA1 SR interneurons. (A) U-tube application of ACh induced NMDA EPSCs. After 10 min exposure of the slice to 1 μM mecamylamine, ACh induced fewer NMDA EPSCs. (B) In another neuron, ACh-induced NMDA EPSCs were abolished after 10 min exposure of the slice to 1 mM choline. (C) Quantification of the inhibitory effects of mecamylamine and choline on ACh-induced EPSCs. The net charge of ACh-induced NMDA EPSCs in presence of the drugs was compared to the average response of control and wash (n = 4 for MEC, and 2 for choline). [a]$p < 0.006$ by one sample t-test. Membrane potential = +40 mV.

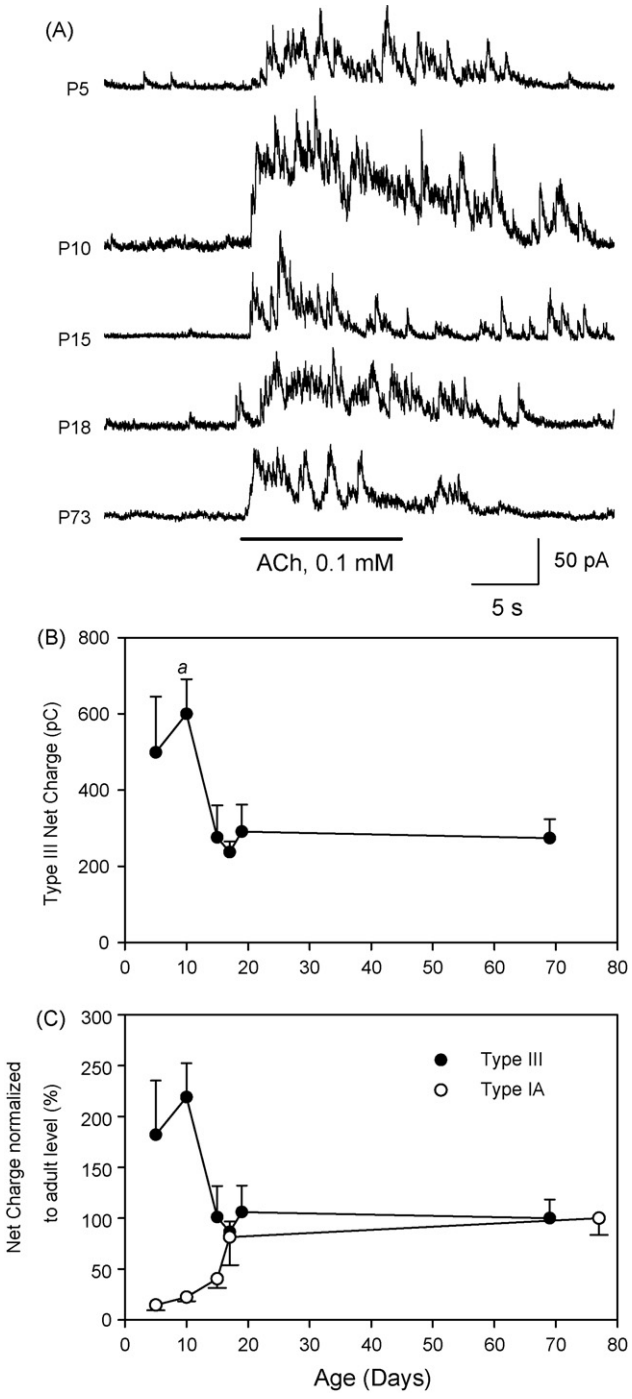

Fig. 5 – Age-dependent changes in the magnitude of type III nAChR responses. (A) Sample traces of ACh-induced NMDA EPSCs recorded from CA1 SR interneurons of hippocampal slices from rats at different ages. Note that the largest response occurred at P10. (B) Plot of the average net charge of ACh-induced NMDA EPSCs from several neurons at different ages. Each symbol and error bars represent mean and SEM, respectively, of results obtained from 152 neurons from 95 rats (n = 8 for P5; 47 for P10; 24 for P15; 48 for P17; 16 for P19; and 9 for P69). [a]$p < 0.01$ P10 compared to P15 and P17 according to nonparametric ANOVA. (C) Comparison of type IA and type III response at different ages. The values were normalized to the adult level.

In our study, we used rats from 5 to 141 days after birth, which allowed for an evaluation of nAChR activity from the neonatal period to young adulthood. Thus, this study is the first to assess both $\alpha7^*$ and $\alpha3\beta4\beta2^*$ nAChR responses in the adult rat hippocampal interneurons. The strong similarity in the properties of $\alpha7^*$ and $\alpha3\beta4\beta2^*$ nAChRs in neonatal and young adult rats makes the neonatal hippocampal slice a valid experimental preparation for the testing of clinically relevant

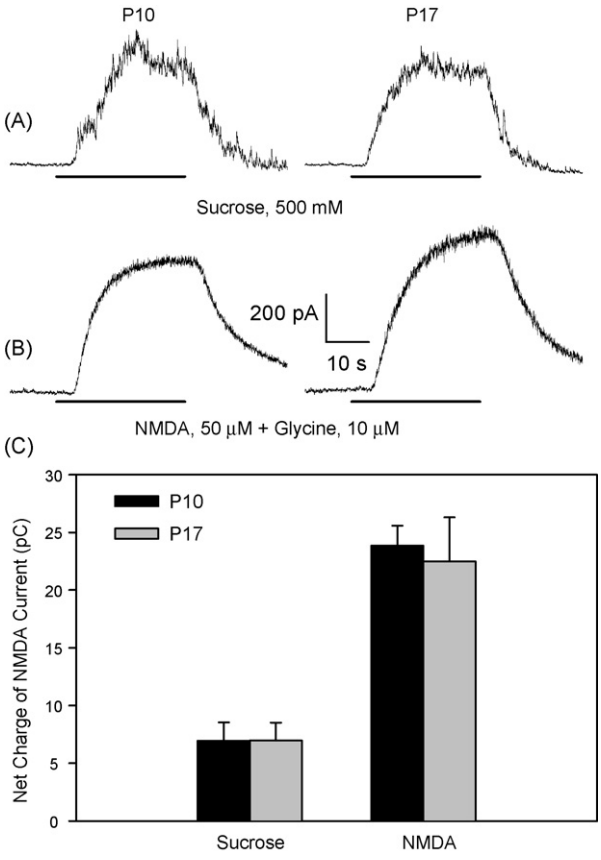

Fig. 6 – NMDA-evoked currents and sucrose-induced NMDA EPSCs in CA1 SR interneurons of hippocampal slices from rats at different ages. (A) U-tube application of Sucrose induced multiple NMDA EPSCs that superimposed to produce an outward current. (B) Outward current evoked by U-tube application of NMDA and glycine. Membrane potential = +40 mV. (C) Summary of the magnitude of sucrose- and NMDA-evoked responses from several neurons. Graph and bars represent mean and SEM, respectively, of results obtained from 5 neurons from 4 rats for sucrose and 4 neurons from 3 rats for NMDA.

nAChR ligands for potential use in adults. It is worth noting that the authors of a recent study [18] used young adult (3 months old) and aged (25–30 months old) rats to assess nAChR function by studying cholinergic afferent stimulated- or cytisine-stimulated GABAergic IPSCs in pyramidal neurons. However, the use of a combination of pharmacological antagonists precluded the identification of specific nAChR subtypes.

The age-dependent increase in the α7* nAChR activity recorded from CA1 SR interneurons is likely to have resulted from an increase in the density of receptors. Previous analysis of levels of mRNA coding for the α7 subunit [20,27,28] or α-bungarotoxin binding autoradiography [20,21] had suggested that the expression of α7 nAChRs in the hippocampus decreases, rather than increases with the age of the rats. The apparent discrepancy between the age-dependent increase in α7* nAChR activity and the age-dependent reduction in α-BGT-binding sites in the rat hippocampus could be reconciled by the higher sensitivity of the electrophysiological measures taken from single neurons compared to the autoradiographic measures. The following explanations should also be considered: (i) the density of functional α7* nAChRs increase in individual interneurons as observed here, but the number of α7 nAChR-expressing interneurons declines during normal development and aging; (ii) autoradiographic measures primarily represent presynaptic α7* nAChRs located on glutamate terminals [21] rather than the postsynaptic receptors located on the interneurons; and/or (iii) the age-dependent increase in α7* nAChR activity reflects age-related changes in intracellular mechanisms that increase α7* nAChR activity. Because the axons of SR interneurons were seen in both SR and SO regions (see Section 3), activation of α7* nAChRs in SR interneurons is likely to modulate the excitability of both apical and basal dendrites of CA1 pyramidal neurons in the mature hippocampus.

The age-dependent increase in α7* nAChR activity in the SR interneurons followed very closely the development of cholinergic afferents in the hippocampus, both components reaching near adult levels during third postnatal week [29]. This coincidental pattern suggests that the cholinergic neurotransmitter ACh uses the α7* nAChR as a postsynaptic partner in the hippocampus, particularly in rats more than 3 weeks old. This concept is supported by the previous demonstration of α7* nAChR-mediated synaptic currents in CA1 SR interneurons [30–32] or γ oscillations in hippocampal slices [33]. Further, the presence of robust α7* nAChR currents in the CA1 SR interneurons of adult rats is consistent with the described role of hippocampal α7* nAChRs in theta oscillations [19] and memory [34] in adult rats. α7* nAChRs have been implicated in the induction of long-term potentiation (LTP) in brain reward areas [35] and in the hippocampus [36]. There are reports that in rats the endurance of hippocampal LTP increases with age, with adult level of persistent LTP being reached in the third postnatal week [37]. The parallel age-dependent increase in LTP in the hippocampus and functional α7* nAChRs in CA1 SR interneurons lead to the hypothesis that the two events are related to each other.

In addition to being regulated by somatodendritic α7* nAChRs, the excitability of CA1 SR interneurons in the immature [12] and the mature (this study) hippocampus can be regulated by glutamatergic neurons/axons expressing α3β4β2* nAChRs. The age-dependent reduction in α3β4β2* nAChR-dependent modulation of glutamate release onto the CA1 SR interneurons suggests that type III nAChRs rather than α7* nAChRs play a dominant role in controlling the excitation of SR interneurons in the immature hippocampus. The second postnatal week is the most sensitive developmental period for the disruptive action of nicotine on the NMDA component of glutamate synaptic transmission [38,39]. Thus, it is conceivable that type III nAChR is a major target for nicotine during this critical developmental period. This is also supported by the observations that type III nAChR is the most sensitive among the hippocampal nAChR subtypes to the desensitizing action of nicotine, and is readily upregulated by one or two injections of nicotine at P14-P15 [12]. Since functional type III nAChR, sensitive to inhibition by choline [13], are present on glutamate axons during the first postnatal week, when choline uptake mechanisms are not fully developed [40], the activity of

this receptor can be modulated by endogenous levels of choline.

In conclusion, the present study demonstrates that the magnitude of nAChR responses recorded from CA1 SR interneurons changes significantly with the age of rats, from early postnatal days to adulthood, in a receptor subtype-dependent manner. This may represent a mechanism by which two pharmacologically distinct nAChR subtypes regulate the excitability of the same interneuron at different ages.

Acknowledgements

We thank Mabel Zelle for technical assistance and for editing the manuscript. We are thankful to Bhagavathy Alkondon for preparing hippocampal slices and for Neurolucida drawing of neurons. This work was supported by the United States Public Health Service Grants NS41671 and NS25296.

REFERENCES

[1] Lukas RJ, Changeux JP, Le Novere N, Albuquerque EX, Balfour DJ, Berg DK, et al. International Union of Pharmacology. XX. Current status of the nomenclature for nicotinic acetylcholine receptors and their subunits. Pharmacol Rev 1999;51:397–401.
[2] Dani JA, Bertrand D. Nicotinic acetylcholine receptors and nicotinic cholinergic mechanisms of the central nervous system. Ann Rev Pharmacol Toxicol 2007;47: 699–729.
[3] Liu Z, Neff RA, Berg DK. Sequential interplay of nicotinic and GABAergic signaling guides neuronal development. Science 2006;314:1610–3.
[4] Lindstrom J. Nicotinic acetylcholine receptors of muscles and nerves: comparison of their structures, functional roles, and vulnerability to pathology. Ann N Y Acad Sci 2003;998:41–52.
[5] Albuquerque EX, Alkondon M, Pereira EFR, Castro NG, Schrattenholz A, Barbosa CTF, et al. Properties of neuronal nicotinic acetylcholine receptors: pharmacological characterization and modulation of synaptic function. J Pharmacol Exp Ther 1997;280:1117–36.
[6] Lena C, Changeux JP, Mulle C. Evidence for "preterminal" nicotinic receptors on GABAergic axons in the rat interpeduncular nucleus. J Neurosci 1993;13:2680–8.
[7] Lester RA, Dani JA. Acetylcholine receptor desensitization induced by nicotine in rat medial habenula neurons. J Neurophysiol 1995;74:195–206.
[8] Alkondon M, Pereira EFR, Eisenberg HM, Albuquerque EX. Choline and selective antagonists identify two subtypes of nicotinic acetylcholine receptors that modulate GABA release from CA1 interneurons in rat hippocampal slices. J Neurosci 1999;19:2693–705.
[9] Frazier CJ, Rollins YD, Breese CR, Leonard S, Freedman R, Dunwiddie TV. Acetylcholine activates an α-bungarotoxin-sensitive nicotinic current in rat hippocampal interneurons, but not pyramidal cells. J Neurosci 1998;18:1187–95.
[10] Jones S, Yakel JL. Functional nicotinic ACh receptors on interneurons in the rat hippocampus. J Physiol 1997;504:603–10.
[11] Alkondon M, Albuquerque EX. The nicotinic acetylcholine receptor subtypes and their function in the hippocampus and cerebral cortex. Prog Brain Res 2004;145:109–20.
[12] Alkondon M, Albuquerque EX. Nicotinic receptor subtypes in rat hippocampal slices are differently sensitive to desensitization and early in vivo functional up-regulation by nicotine and to block by bupropion. J Pharmacol Exp Ther 2005;313:740–50.
[13] Alkondon M, Albuquerque EX. Subtype-specific inhibition of nicotinic acetylcholine receptors by choline: a regulatory pathway. J Pharmacol Exp Ther 2006;318:268–75.
[14] Alkondon M, Pereira EFR, Albuquerque EX. NMDA and AMPA receptors contribute to the nicotinic cholinergic excitation of CA1 interneurons in the rat hippocampus. J Neurophysiol 2003;90:1613–25.
[15] Hoyle E, Genn RF, Fernandes C, Stolerman IP. Impaired performance of α7 nicotinic receptor knockout mice in the five-choice serial reaction time task. Psychopharmacology 2006;189:211–23.
[16] Freedman R, Hall M, Adler LE, Leonard S. Evidence in postmortem brain tissue for decreased numbers of hippocampal nicotinic receptors in schizophrenia. Biol Psychiatry 1995;38:22–33.
[17] De Rover M, Mansvelder HD, Lodder JC, Wardeh G, Schoffelmeer ANM, Brussaard AB. Long-lasting nicotinic modulation of GABAergic synaptic transmission in the rat nucleus accumbens associated with behavioural sensitization to amphetamine. Eur J Neurosci 2004;19: 2859–70.
[18] Potier B, Jouvenceau A, Epelbaum J, Dutar P. Age-related alterations of GABAergic input to CA1 pyramidal neurons and its control by nicotinic acetylcholine receptors in rat hippocampus. Neuroscience 2006;142:187–201.
[19] Siok CJ, Rogers JA, Kocsis B, Hajós M. Activation of α7 acetylcholine receptors augments stimulation-induced hippocampal theta oscillation. Eur J Neurosci 2006;23:570–4.
[20] Adams CE, Broide RS, Chen Y, Winzer-Serhan UH, Henderson TA, Leslie FM, et al. Development of the α7 nicotinic cholinergic receptor in rat hippocampal formation. Brain Res Dev Brain Res 2002;139:175–87.
[21] Tribollet E, Bertrand D, Marguerat A, Raggenbass M. Comparative distribution of nicotinic receptor subtypes during development, adulthood and aging: an autoradiographic study in the rat brain. Neuroscience 2004;124:405–20.
[22] Zhang X, Liu C, Miao H, Gong ZH, Nordberg A. Postnatal changes of nicotinic acetylcholine receptor α2, α3, α4, α7 and β2 subunits genes expression in rat brain. Int J Dev Neurosci 1998;16:507–18.
[23] Alkondon M, Albuquerque EX. Nicotinic acetylcholine receptor α7 and α4β2 subtypes differentially control GABAergic input to CA1 neurons in rat hippocampus. J Neurophysiol 2001;86:3043–55.
[24] Alkondon M, Albuquerque EX. A non-α7 nicotinic acetylcholine receptor modulates excitatory input to hippocampal CA1 interneurons. J Neurophysiol 2002;87:1651–4.
[25] Rosenmund C, Stevens CF. Definition of the readily releasable pool of vesicles at hippocampal synapses. Neuron 1996;16:1197–207.
[26] Ashton AC, Ushkaryov YA. Properties of synaptic vesicle pools in mature central nerve terminals. J Biol Chem 2005;280:37278–8.
[27] Broide RS, O'Connor LT, Smith MA, Smith JAM, Leslie FM. Developmental expression of α7 neuronal nicotinic receptor messenger RNA in rat sensory cortex and thalamus. Neuroscience 1995;67:83–94.
[28] Shacka JJ, Robinson SE. Postnatal developmental regulation of neuronal nicotinic receptor subunit α7 and multiple α4 and β2 mRNA species in the rat. Brain Res Dev Brain Res 1998;109:67–75.

[29] Aznavour N, Watkins KC, Descarries L. Postnatal development of the cholinergic innervation in the dorsal hippocampus of rat: quantitative light and electron microscopic immunocytochemical study. J Comp Neurol 2005;486:61–75.
[30] Alkondon M, Pereira EFR, Albuquerque EX. α-bungarotoxin- and methyllycaconitine-sensitive nicotinic receptors mediate fast synaptic transmission in interneurons of rat hippocampal slices. Brain Res 1998;810:257–63.
[31] Frazier CJ, Buhler AV, Weiner JL, Dunwiddie TV. Synaptic potentials mediated via α-bungarotoxin-sensitive nicotinic acetylcholine receptors in rat hippocampal interneurons. J Neurosci 1998;18:8228–35.
[32] Hefft S, Hulo S, Bertrand D, Muller D. Synaptic transmission at nicotinic acetylcholine receptors in rat hippocampal organotypic cultures and slices. J Physiol (Lond) 1999;515:769–76.
[33] Song C, Murray TA, Kimura R, Wakui M, Ellsworth K, Javedan SP, et al. Role of α7-nicotinic acetylcholine receptors in titanic stimulation-induced γ oscillations in rat hippocampal slices. Neuropharmacology 2005;48:869–80.
[34] Nott A, Levin ED. Dorsal hippocampal α7 and α4β2 nicotinic receptors and memory. Brain Res 2006;1081:72–8.
[35] Mansvelder HD, McGehee DS. Long-term potentiation of excitatory inputs to brain reward areas by nicotine. Neuron 2000;27:349–57.
[36] Chen L, Yamada K, Nabeshima T, Sokabe M. α7 nicotinic acetylcholine receptor as a target to rescue deficit in hippocampal LTP induction in β-amyloid infused rats. Neuropharmacology 2006;50:254–68.
[37] Jackson PS, Suppes T, Harris KM. Stereotypical changes in the pattern and duration of long-term potentiation expressed at postnatal days 11 and 15 in the rat hippocampus. J Neurophysiol 1993;70:1412–9.
[38] Aramakis VB, Hsieh CY, Leslie FM, Metherate R. A critical period for nicotine-induced disruption of synaptic development in rat auditory cortex. J Neurosci 2000;20:6106–16.
[39] Hsieh CY, Leslie FM, Metherate R. Nicotine exposure during a postnatal critical period alters NR2A and NR2B mRNA expression in rat auditory forebrain.. Brain Res Dev Brain Res 2002;133:19–25.
[40] Klein J, Weichel O, Ruhr J, Dvorak C, Löffelholz K. A homeostatic mechanism counteracting K^+-evoked choline release in adult brain. J Neurochem 2002;80:843–9.
[41] Alkondon M, Pereira EFR, Barbosa CTF, Albuquerque EX. Neuronal nicotinic acetylcholine receptor activation modulates γ-aminobutyric acid release from CA1 neurons of rat hippocampal slices. J Pharmacol Exp Ther 1997;283:1396–411.
[42] McQuiston AR, Madison DV. Nicotinic receptor activation excites distinct subtypes of interneurons in the rat hippocampus. J Neurosci 1999;19:2887–96.
[43] Sudweeks SN, Yakel JL. Functional and molecular characterization of neuronal nicotinic ACh receptors in rat CA1 hippocampal neurons. J Physiol 2000;527:515–28.
[44] Buhler AV, Dunwiddie TV. α7 nicotinic acetylcholine receptors on GABAergic interneurons evoke dendritic and somatic inhibition of hippocampal neurons. J Neurophysiol 2002;87:548–57.
[45] Maggi L, Magueresse CL, Changeux JP, Cherubini E. Nicotine activates immature ''silent'' connections in the developing hippocampus. Proc Natl Acad Sci 2003;100:2059–64.
[46] Thinschmidt JS, Frazier CJ, King MA, Meyer EM, Papke RL. Septal innervation regulates the function of α7 nicotinic receptors in CA1 hippocampal interneurons. Exp Neurol 2005;195:342–52.
[47] Chang Q, Fischbach GD. An acute effect of neuregulin 1β to suppress α7- containing nicotinic acetylcholine receptors in hippocampal interneurons. J Neurosci 2006;26:11295–303.
[48] Alkondon M, Pereira EFR, Potter MC, Kauffman FC, Schwarcz R, Albuquerque EX. Strain-specific nicotinic modulation of glutamatergic transmission in the CA1 field of the rat hippocampus: August Copenhagen Irish versus Sprague-Dawley. J Neurophysiol 2007;97:1163–70.